ICRH operations and experiments during the JET-ILW tritium and DTE2 campaigns

ICRH Operations and Experiments During the JET-ILW Tritium and DTE2 Campaigns

P. Jacquet[1,a)], E. Lerche[1,2], M. Mantsinen[3,4], D. Van Eester[2], K. Kirov[1], P. Mantica[5], D. Gallart[3], D. Taylor[1], Y. Kazakov[2], I. Monakhov[1], C. Noble[1], P. Dumortier[2], H. Sheikh[1], C. Challis[1], J. Hobirk[6], A. Kappatou[6], M. Maslov[1], D. King[1], D. Keeling[1], F. Rimini[1], D. Frigione[7], L. Garzotti[1], P. Lomas[1], C. Lowry[8], I. Carvalho[1], M. Baruzzo[9], C. Reux[10], M. Lenholm[1], R. Henriques[1], E. De la Luna[11], J. Mailloux[1], C. Maggi[1], J. Garcia[10], A. Chomiczewska[12], W. Gromelski[12], V. Bobkov[6], D. Milanesio[13], L. Colas[10], W. Tierens[6], R. Otin[1], C. Klepper[14], E. Delabie[14], R. Dumont[10], J. Eriksson[15], V. Kiptily[1], S. Menmuir[1], M. Nocente[16], A. Patel[1], G. Pucella[9], D. Rigamonti[5], M. Tardochi[5], S. Silburn[1], P. Siren[1], E. Solano[11], Z. Stancar[1,17], M. Valisa[18], D. Douai[10], D. Matveev[19], T. Wauters[20], and JET contributors.

[1]UKAEA, CCFE, Culham Science Centre, Abingdon, Oxon, OX14 3DB, UK
[2]Laboratory for Plasma Physics, ERM/KMS, B-1000 Brussels, Belgium
[3]Barcelona Supercomputing Center, Barcelona, Spain
[4]ICREA, Barcelona, Spain
[5]Institute of Plasma Science and Technology, CNR, 20125 Milano, Italy
[6]Max-Planck-Institut für Plasmaphysik, Boltzmannstr. 2, 85748 Garching, Germany
[7]University of Tor Vergata, Rome, Italy
[8]European Commission, B-1049 Brussels, Belgium.
[9]ENEA, Fusion and Nuclear Safety Department, C.R. Frascati, 00044 Frascati, Italy
[10]CEA, IRFM, F-13108 St-Paul-Lez-Durance, France
[11]Laboratorio Nacional de Fusión, CIEMAT, 28040 Madrid, Spain
[12]Institute of Plasma Physics and Laser Microfusion, Hery 23, 01-497 Warsaw, Poland
[13]Politecnico di Torino, Torino, Italy
[14]Oak Ridge National Laboratory, Oak Ridge, Tennessee, TN 37830, USA
[15]Department of Physics and Astronomy, Uppsala University, 75120 Uppsala, Sweden
[16]Dipartimento di Fisica 'G. Occhialini', Universit`a di Milano-Bicocca, Milano, Italy
[17]Slovenian Fusion Association (SFA), Jozef Stefan Institute, SI-1000 Ljubljana, Slovenia
[18]Consorzio RFX, 35127 Padova, Italy
[19]Forschungszentrum Jülich GmbH, Institut für Energie- und Klimaforschung-Plasmaphysik, 52425, Jülich, Germany
[20]ITER Organization, 13067 St Paul Lez Durance, France

[a)]Corresponding author:philippe.jacquet@ukaea.uk

Abstract. 2021 has culminated with the completion of the JET-ILW DTE2 experimental campaign. This contribution summarizes Ion Cyclotron Resonance Heating (ICRH) operations from system and physics point of view. Improvements to the (ICRH) system, to operation procedures and to real time RF power control were implemented to address specific constraints from tritium and deuterium-tritium operations and increase the system reliability and power availability during D-T pulses. ICRH was operated without the ITER-Like Antenna (ILA) because water leaked from an in-vessel capacitor into the vessel on day-2 of the D-T campaign. Three weeks were required to identify and isolate the leak and resume plasma operations. Dedicated RF-Plasma Wall Interaction (PWI) experiments were conducted; tritium plasmas exhibit a higher level of Be sputtering on the outer wall and impurity content when compared to deuterium or hydrogen plasmas. The JET-DTE2 campaigns provided the opportunity to characterize ICRH schemes foreseen for the ITER operation, in the ITER like wall environment in ELMy H-mode scenarios aiming at maximizing fusion performance. The second harmonic tritium resonance heating and to a lesser extent minority ^{3}He heating (ITER D-T ICRH reference schemes) lead to improved ion temperature and fusion performance when compared to hydrogen minority ICRH. However, these discharges suffered from a lack of stationarity and gradual impurity accumulation potentially because of a deficit of ICRH power when using JET antennas at lower frequencies. Fundamental deuterium ICRH was used in tritium-rich plasmas and with deuterium Neutral Beam Heating; this ICRH scheme proved to be very efficient boosting ion temperature and fusion performance in these plasmas.

INTRODUCTION

An experimental campaign with Tritium (T) and Deuterium-Tritium (D-T) plasmas was run on JET-ITER-Like Wall (JET-ILW) in 2021-2022. This JET-DTE2 campaign was a unique opportunity to address essential questions for magnetic fusion development, and in particular to prepare for ITER operations and experiments. The JET-DTE2 objectives were:

- Demonstrate fusion power from 10 MW up to 15MW, sustained for 5s.
- Demonstrate integrated radiative scenarios in plasma conditions relevant to ITER.
- Demonstrate clear α-particle effects.
- Clarify isotope effects on energy and particle transport and explore consequences of mixed species plasmas.
- Address key Plasma-Wall Interaction issues.
- Demonstrate RF schemes relevant to ITER D-T operation.
- Demonstrate Tritium Removal.

To deliver the above objectives, ICRH was used in most JET-DTE2 and tritium plasmas to provide electron heating [1,2] for central impurities chase out and discharges stationarity. ICRH was also used for bulk heating of fuel ions and boost fusion power. Specific experiments were performed to study the impact of isotopes on RF induced Plasma Wall Interactions (PWI). The demonstration of ITER D-T ICRH scenarios was one of the items of the JET-DTE2 program. Finally, Ion Cyclotron Wall Cleaning (ICWC) was an element of the tritium cleaning strategy. This paper will describe constraints from tritium and deuterium-tritium plasmas on ICRH operations. Then we will summarize experiments characterizing the impact of tritium plasmas on RF specific PWI. Finally, results from dedicated experiments aiming at demonstrating ITER D-T ICRH scenarios in high performance H-mode plasmas will be briefly reported.

ICRH OPERATIONS

A top view of JET with the auxiliary heating systems is shown in Figure 1. A description of the system can be found in [3,4]. The A2 antennas A, B, C and D were used during JET-DTE2. To provide ELM resilience A&B are fed via a 3 dB hybrid couplers network, while C&D are fed via an External Conjugate-T network (ECT); C&D can also be fed independently. In preparation for the tritium and D-T campaign a program of improvement of the JET ICRH system was implemented over several years. This was driven essentially by:

(a) Tritium safety constraints: to prevent tritium permeating through the vacuum windows from accumulating into the transmission lines, the following activities were performed: systematic check of the bleeding flow from the ICRH transmission lines to the JET gas collection system; check of the satisfactory operation of the emergency

isolation valves; identification and repair of transmission lines air leaks; improvement of the distribution system and modification of the venting procedure (venting through the JET Active Gas Handling System). Also, any breach to the transmission lines is now subject to a Health-Physics survey.

(b) Radiological safety constraints: the generators area could not be accessed when JET was running in D-T; hence, a number of projects were conducted to improve the reliability of the plant and enhance capabilities to control and monitor the ICRH plant remotely.

ICRH was used in ~80% of JET-DTE2 campaign pulses. Figure 2 shows the launched power vs frequency in DTE2 ICRH pulses. Almost the whole available frequency range for the ICRH system on JET (23-57 MHz) was used. Also noticeable, the maximum launched power achieved is lower for lower frequencies; this is caused by the reduced coupling resistance at lower frequencies for the JET A2 antennas. At ~25 MHz/55 MHz, extra limitations arise because mechanical matching elements in the RF generators are at the end of their range.

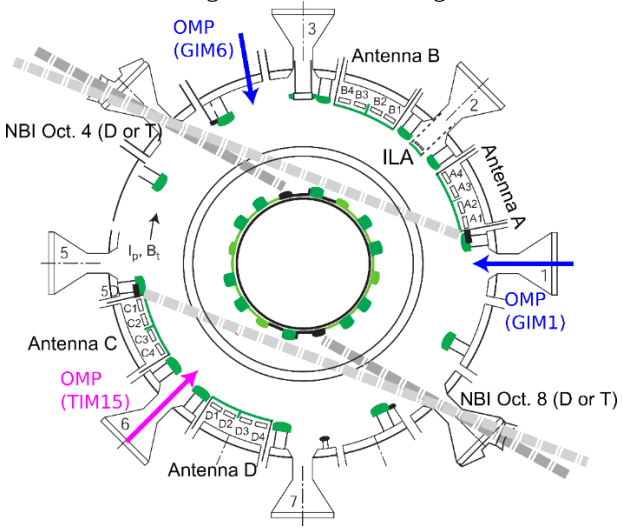

FIGURE 1. Top View of JET showing the NBI and ICRH auxiliary heating systems. Also shown are the Outer Mid-Plane (OMP) gas injection modules (TIMs for tritium, GIMs for deuterium) used in the hybrid scenario experiments described later in the paper.

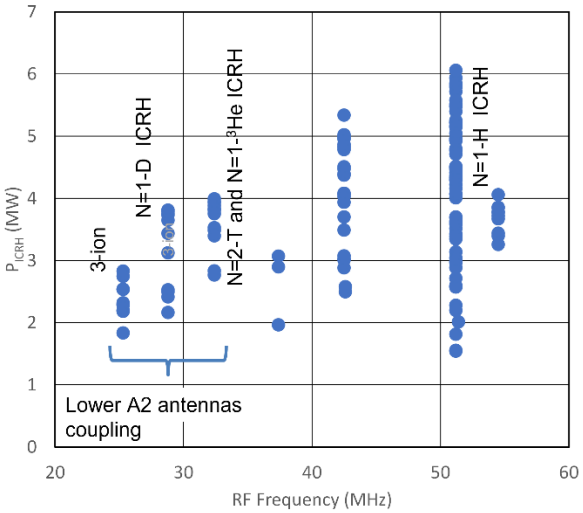

FIGURE 2. ICRH launched power plotted as a function of frequency during the DTE2 campaign. Typical ICRH scheme usage in DTE2 vs frequency is also indicated.

To maximize the outcomes of the T and D-T campaigns while not exceeding the allocated T and neutron budgets, the procedure to prepare the system before a discharge was also improved. The target was to get the required coupled ICRH power on the first pulse of the day. Each frequency change was systematically followed by test load pulses to verify the state of the generators and identify limits if any, so that appropriate actions can be taken before an actual D-T pulse is performed. Reference pulses (with adequate plasma conditions) to set the position of the matching elements were systematically used. The program that handles real time control of the generators was improved as recommended in [5]. The control scheme aims at delivering the required launched power (or maximum power given antenna coupling and generator limits) while minimizing the risk of trips; typically, trips can arise when breakdown are detected in the transmission lines or at the antennas or when generators current/voltage limits are exceeded. The algorithm equalizes the transmission line voltages for an antenna pair and ensures that the voltages are kept below preset limits (exceeding those limits would result in increased risk of arcing). If relevant, generators power limits are also considered. This algorithm ensures maximum power delivery to the plasma given the antenna coupling (plasma conditions dependent) and limitations (potentially due to faults) of the RF system. An example of the new control algorithm operation in an ELMy H-mode plasma is shown in Figure 3. In this example, antenna C&D coupling resistance is higher (RF-voltages on C&D not quite at the limit); this is partly because the Tritium Injection Module TIM15 (shown in Figure 1) located between antennas C and D is used, hence $P_{ICRH,C\&D} > P_{ICRH,A\&B}$.

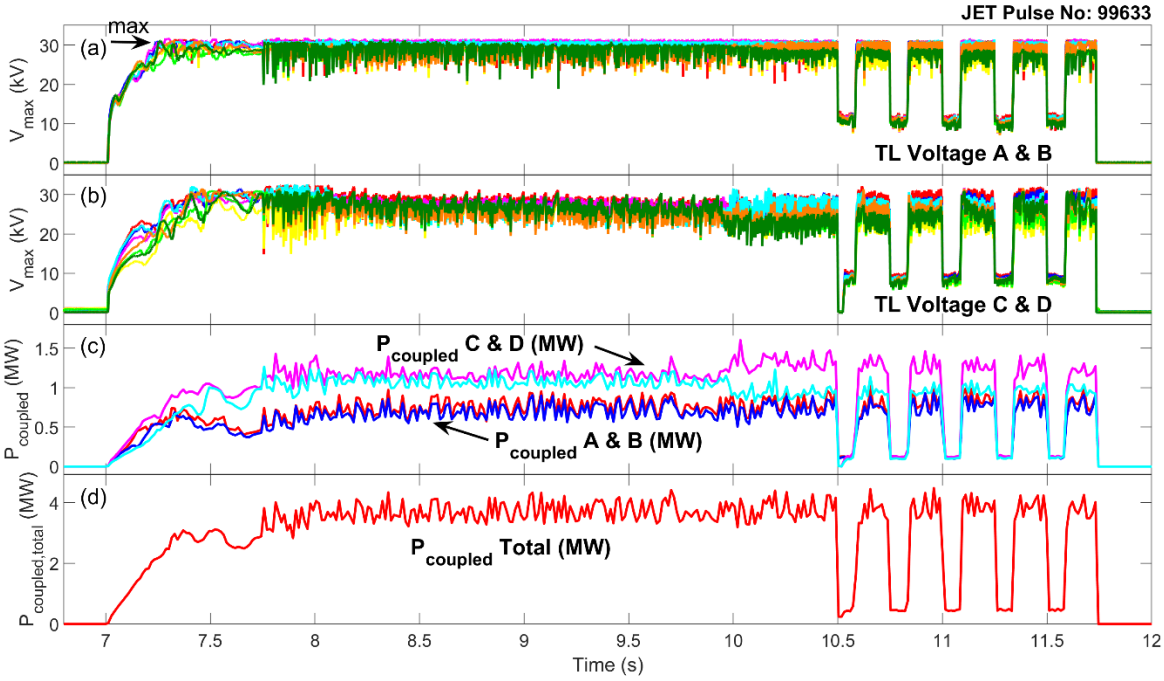

FIGURE 3. Example showing real time optimization of RF voltages in the transmission lines feeding the A2 antennas to maximize the ICRH launched power. Pulse 99633 with I_P=2.3MA, B_T=3.45T, ^{3}He minority ICRH with f_{RF}=32.5MHz. (a) RF-Voltages in the 8 transmission lines feeding antennas A&B (fed via 3dB-hybrid couplers). RF amplifiers power is adjusted so RF-voltages reach the maximum permissible, 30 kV. (b) RF-Voltages in the 8 transmission lines feeding antennas C&D (fed via ECTs). (c) power launched by antennas A&B, and C&D. (d) total ICRH power.

In September 2020, one of the ITER Like Antenna (ILA) [6] capacitors failed (C2 from ILA upper row). Figure 4 represents a sketch of a capacitor cooling circuit. The capacitor filled-in with water after a micro-leak developed in the bellow between the water-cooling circuit and the capacitor. In the autumn 2020 a differential pumping system was installed to evacuate the upper row capacitors water cooling circuits. Operations with the ILA lower row resumed in January 2021, but in August 2021 a second fault developed on day-2 of the JET-DTE2 campaign. Some water was still being retained in C2; during a pulse, a crack developed either in the capacitor ceramic or in the brazing joint, and the water was released to the JET vacuum vessel. It took three weeks to identify the origin of the leak into the JET torus, to fully evacuate the water and recondition the machine before JET operations could resume. As a precaution, the ILA was not run during the DTE2 campaign; but the lower row of the antenna has been operated again afterwards. The ability to drain, fill, inject marker gases and isolate/pump the different ILA water cooling circuits separately was crucial to localize the faulty cooling circuit. The differential pumping system installed in the autumn 2020 presently mitigates the effect of this double fault in C2 and allows JET to run.

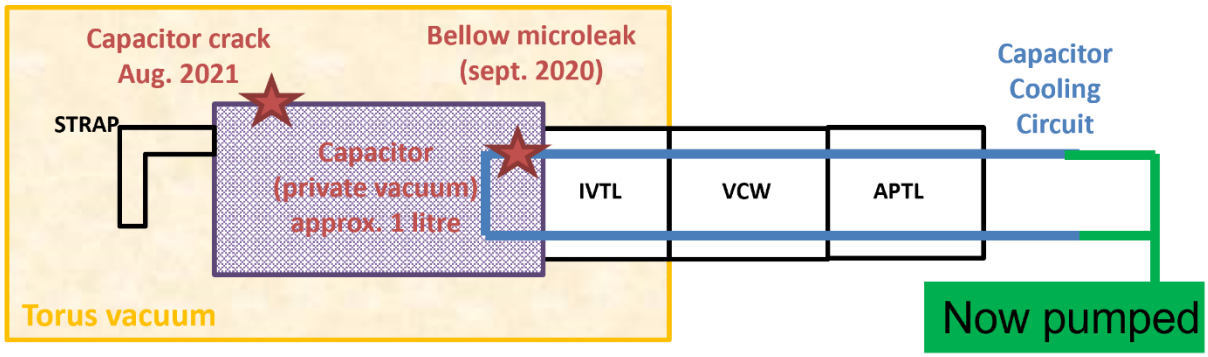

FIGURE 4. Simplified diagram of ILA capacitors cooling circuit and vacuum arrangement showing the suspected location of the faults leading to a water leak into the JET vessel.

RF SPECIFIC PWI IN TRITIUM PLASMAS

Although ICRH is a principal tool used to prevent core W accumulation in JET plasmas, application of RF power usually leads to an overall increase of the plasma impurity content, and in particular in JET-ILW, tungsten (W) and nickel (Ni) [7]. This is in general attributed to an enhanced Plasma Wall Interaction (PWI) and to sputtering of the Plasma Facing Components (PFC) when applying ICRH. Numerous studies have linked RF sheath rectification [8,9] and the sputtering of the limiters close to or magnetically connected to the active antennas (see for example [10,11]).

Experiments were conducted to assess the effect of plasma isotopes on RF-PWI. In the example given here, we repeated in tritium plasmas deuterium references where we monitored impurity concentration (Ni and W) and Be line emission from the Outer Poloidal Limiters-OPL (see Figure 5). The hydrogen minority ICRH scheme was used in these pulses. Both pulses were run with antenna D only, dipole strap phasing, with 1MW ICRH launched power in the Deuterium case and 0.5 MW in the Tritium case (higher power would saturate Be-line spectroscopy in the tritium plasmas). During the pulses, the fraction of power from the inner straps of the antenna was scanned to find a minimum in impurity production. The Be sputtering yield on the OPLs is higher in tritium plasmas as is the Ni concentration (and also W, not shown) in the plasma. Based on previous JET experiments [12] we attribute the increased impurity content in the plasma to an increase of the source. Work is ongoing to understand the cause of these enhanced RF-PWI observed in tritium plasmas. Modelling of JET A2 antennas with the antenna code TOPICA [13] was performed for these pulses using the measured density profiles in these deuterium or tritium plasmas; calculations do not show increased RF $E_{//}$ fields in front of the antennas with tritium plasmas ($E_{//}$ fields are the drivers of RF-Sheath rectification, see for example [12]). Different hypotheses are under consideration, for example invoking slow wave properties in the SOL and larger RF-sheath rectification with tritium, or an increased Be sputtering yield by tritium.

Experiments were also conducted when using the ^{3}He minority ICRH scheme in hydrogen, deuterium, or tritium plasmas. RF-PWI are enhanced in D and T plasmas (when compared to H); analysis and comparison between D and T is still ongoing, the ^{3}He concentration also having an impact on the Be sputtering. A detailed report will be the subject of future publications.

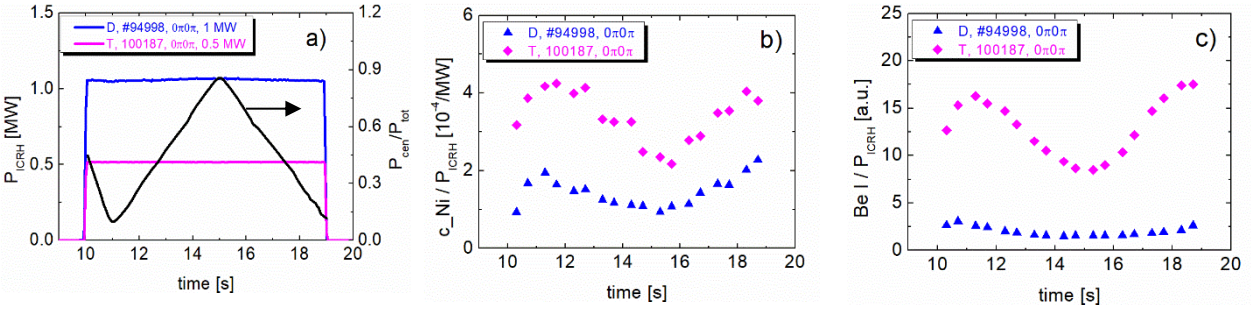

FIGURE 5. Comparison of RF-PWI for a D reference pulse (#94998) repeated with T plasma (#100187). Pulses with I_P=1.8MA, B_T=3T, f_{RF}=42 MHz. (a) ICRH launched power and fraction of power from the inner straps. (b) plasma Ni concentration from VUV spectroscopy (at ρ~0.85). (c) BeI line emission (normalised to the launched ICRH power), spectroscopy diagnostic line of sight on midplane-OPL next to antenna D.

When using the hydrogen minority ICRH scheme in presence of tritium, the 2nd harmonic tritium resonance ($\omega=2\omega_{c,T}$) is also located in the plasma close to the inner wall (see Figure 6-a). Dedicated pulses with hydrogen minority ICRH in the plasma core were performed, in H-mode tritium plasmas and with tritium NBI to verify that the $\omega=2\omega_{c,T}$ inner wall resonance did not cause adverse heat-loads to the JET wall (I_P=2.5 MA, B_T=2.8 T, f_{RF}=42 MHz, 4 MW ICRH, 24 MW tritium NBI).

TEST OF D-T ICRH SCHEMES FOR ITER

The reference ICRH scenario for D-T experiments on ITER [14, 15, 16] is the 2nd harmonic tritium ICRH ($\omega=2\omega_{c,T}$, f=53 MHz for B_T=5.3T) used in conjunction with minority fundamental ^{3}He ICRH ($\omega=\omega_{c,3He}$). These scenarios were tested in the JET-DTE1 campaign in RF only H-mode plasmas [17,18] and in TFTR [19]; on JET, best ion heating and fusion performance were obtained when ^{3}He with a concentration of ~2% was added in the plasma. The

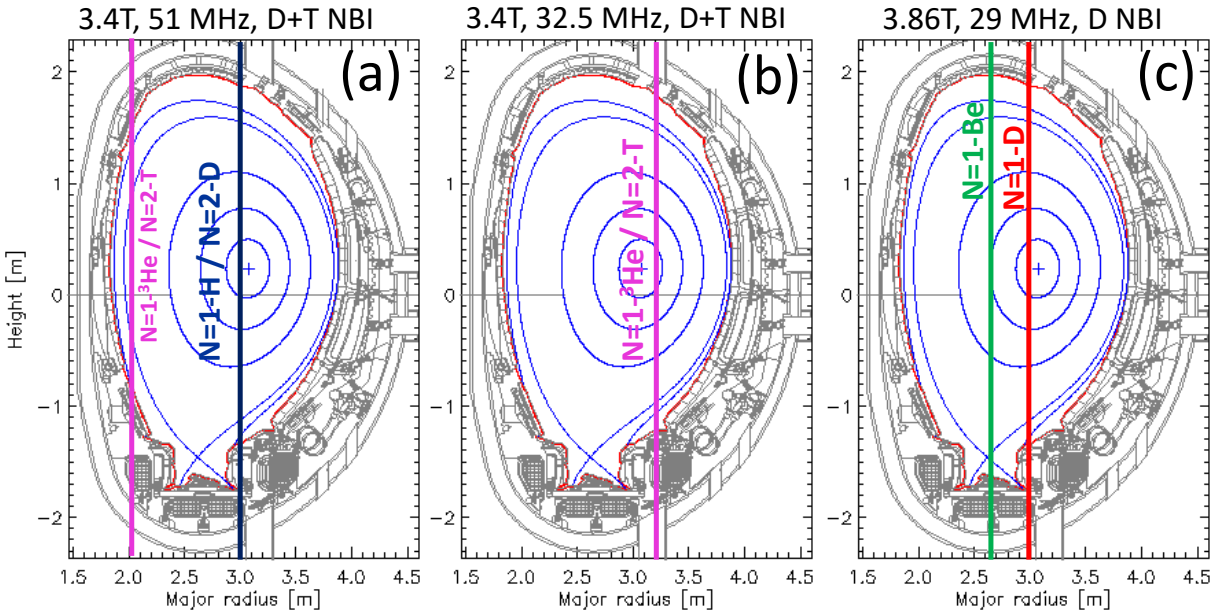

FIGURE 6. JET cross sections showing the resonances position when using different ICRH scenarios in D-T plasmas. (a) $\omega=\omega_{c,H}$ / $\omega=2\omega_{c,D}$ ICRH ; in this case, note the presence of the inner wall resonance $\omega=2\omega_{c,T}$ which did not cause a problem in D-T or tritium plasmas, even with tritium NBI. (b). $\omega=2\omega_{c,T}$ /$\omega=\omega_{c,3He}$ ICRH. (c) $\omega=\omega_{c,D}$ ICRH.

fundamental deuterium ICRH scenario ($\omega=\omega_{c,D}$, f_{RF}=41 MHz for B_T=5.3 T) is also accessible on ITER. Fundamental deuterium ICRH was tested in JET-DTE1 [20] in RF only H-mode plasmas and very good heating and fusion performance were obtained (Q_{fusion}=0.22). These scenarios were revisited in JET-DTE2 in high performance H-mode discharges with high NBI power; one of the objectives of JET-DTE2 was to test and characterize the D-T ICRH schemes for ITER in the JET-ILW environment, in good performance H-mode plasmas, taking advantage of upgraded diagnostics [21,22], including the capability to now resolve ^{3}He down to small fractions of a percent [23]. This is also an opportunity to benchmark modelling tools [24,25,26,27,28,29]. Note that the hydrogen minority scenario (not accessible on ITER full field) which provides dominant collisional electron heating was the work-horse for ICRH in most of JET deuterium, tritium and D-T plasma; it was used for central plasma heating (in particular in the baseline and hybrid scenarios) and as a tool to prevent central impurity (W) accumulation [1,2].

Figure 6 shows the resonance positions when using different ICRH scenarios in JET-DTE2 plasmas. As far as possible a common plasma target was used, the so-called hybrid scenario plasmas [30,31], to ease further analysis and comparisons. The D-T ICRH scenarios for ITER were compared to the hydrogen minority ICRH scenario. In the case of hydrogen minority ICRH, ($\omega=\omega_{c,H}$ / $\omega=2\omega_{c,D}$) the ICRH resonance was located at the plasma center for f_{RF}=51MHz/B_T=3.4T (I_P=2.3 MA). To use $\omega=2\omega_{c,T}$ / $\omega=\omega_{c,3He}$ the exact same plasma conditions were used, and the frequency changed to f_{RF}=32.5 MHz resulting to a slightly low-field-side off-axis resonance position. ^{3}He was injected during the discharges aiming at studying $\omega=\omega_{c,3He}$ ICRH. The standard hybrid scenario used tritium and deuterium NBI heating (NBI energy in the range 85-110 keV). $\omega=\omega_{c,D}$ ICRH was tested in tritium-rich plasmas (T/D~0.8/0.2), with deuterium NBI only [32]; in this case the magnetic field was increased to 3.86T (and I_P increased to 2.5MA) for central deuterium ICRH absorption with f_{RF}=29MHz.

More details on the $\omega=2\omega_{c,T}$ / $\omega=\omega_{c,3He}$ ICRH tests and comparison to hydrogen minority ICRH are presented in Figure 7. As far as possible, all plasma parameters were exactly matched except the RF frequency, the slightly lower RF power at 32.5 MHz (see also Figure 2) and the addition of ^{3}He for $\omega=\omega_{c,3He}$ ICRH. In particular, the level of gas fueling (which is an important parameter driving fusion performance, ELM frequency, impurity behavior and discharge stability) was similar in these discharges. Most hybrid pulses in JET DTE2 suffered from gradual impurity accumulation, sometimes correlated with MHD activity, leading to 'cooling' of the plasma center, as seen on the decreasing electron temperature (T_e) and increasing radiated power (P_{rad}) traces in Figure 7. The $\omega=2\omega_{c,T}$ / $\omega=\omega_{c,3He}$ ICRH pulses were more affected, presumably because of the deficit in P_{RF} and electron heating with respect to the hydrogen minority pulses. Before this happens (t <9.5 sec) the $\omega=\omega_{c,3He}$ ICRH pulse shows similar performance in

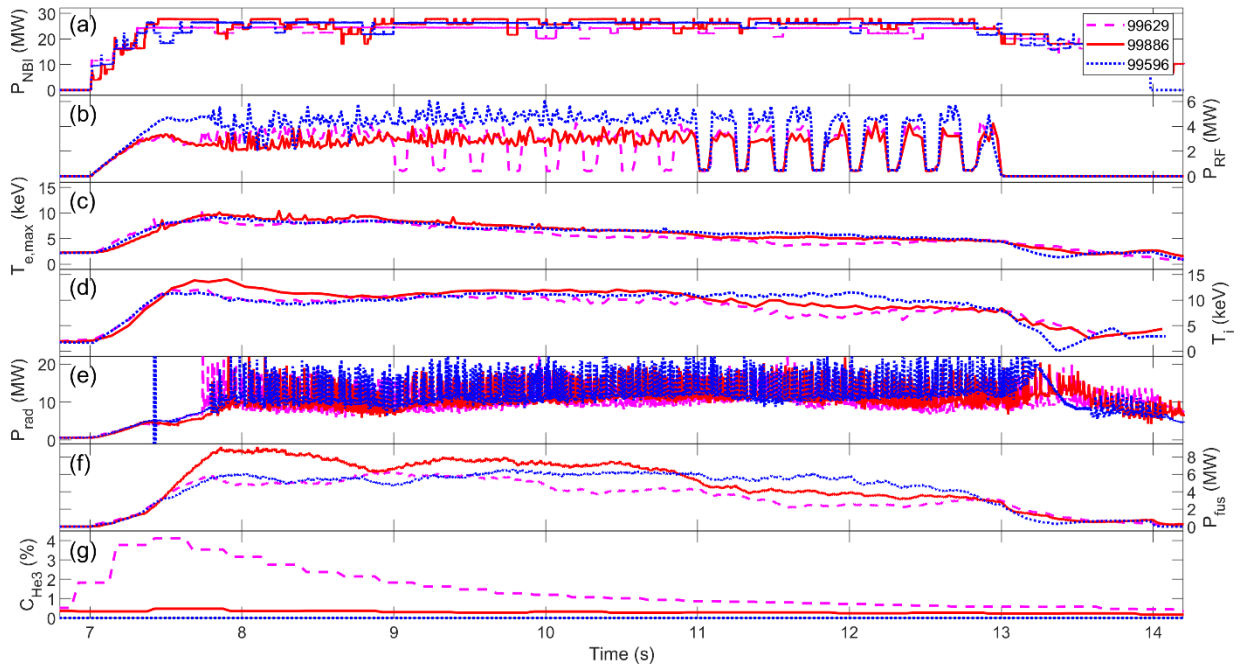

FIGURE 7. Time traces for pulses (I_P=2.3MA, B_T=3,45T) with $\omega=\omega_{c,H,}$ (99596) $\omega=2\omega_{c,T}$ (99886) and $\omega=\omega_{c,3He}$ (99629) ICRH scenarios. (a) NBI power; (b) ICRH power; 4 Hz modulation of P_{RF} was applied for power deposition analysis; (c) electron temperature; (d) ion-temperature, x-Ray crystal spectroscopy; (e) total radiated power, bolometry; (f) fusion power; (g) ^{3}He concentration. In pulse 99629, a ^{3}He puff was injected before turning the RF power ON. The ^{3}He concentration decayed during the high power phase of the pulse to transition from dominant $\omega=\omega_{c,3He}$ heating to mixed $\omega=\omega_{c,3He}$ / $\omega=2\omega_{c,T}$ ICRH.

terms of electron temperature (T_e), ion temperature (T_i) and fusion power as its hydrogen minority counterpart, and the $\omega=2\omega_{c,T}$ ICRH pulse exhibits larger T_i and fusion power.

PION [25], TRANSP-TORIC [26,27], and CYRANO-ETS [28,29] code suites are being used for interpretative analysis of these pulses with different ICRH scenarios. An example illustrating PION simulations is shown in Figure 8 where the RF power absorption profile is shown for $\omega=2\omega_{c,T}$ / $\omega=\omega_{c,3He}$ ICRH pulses and compared to hydrogen minority. In the reference hydrogen minority case, the RF power is absorbed by hydrogen, and also deuterium at the 2nd harmonic. RF accelerated fast hydrogen predominantly redistribute their energy to electrons. In the case of $\omega=\omega_{c,3He}$ ICRH with ~3% ^{3}He the RF power is predominantly absorbed by ^{3}He. When the ^{3}He concentration is reduced, tritium absorption at the 2nd harmonic starts to play a role, direct electron damping also becoming important. In the case of pure $\omega=2\omega_{c,T}$ ICRH (with no ^{3}He), RF power is absorbed by tritium (~42% of the RF power is absorbed by bulk tritium, and ~8% by the NBI tritium), slightly on the low field side, with ~50% of the RF power being absorbed by direct electron damping. Fast ^{3}He and tritium generated by respectively $\omega=\omega_{c,3He}$ and $\omega=2\omega_{c,T}$ ICRH redistribute their energy predominantly on D and T ions. The above picture is confirmed by fast triton measurements by the Neutral Particle Analyzer (NPA) [33] as shown on Figure 9. A fast triton population is observed with pure $\omega=2\omega_{c,T}$ ICRH, but this fast triton tail decreases when ^{3}He is present in the plasma.

An overview of the family of JET-DTE2 pulses using the hybrid scenario as plasma target with different ICRH schemes is shown in Figure 10. The ion temperature, averaged over 8-9 sec., is plotted as a function of the total heating power. As already mentioned, overall the $\omega=2\omega_{c,T}$ ICRH pulses have a higher temperature and enhanced fusion performance (per total input power) when compared to the hybrid pulses with standard H minority ICRH. The $\omega=\omega_{c,3He}$ ICRH pulses also have good T_i and fusion performance. The best fusion performance obtained in the JET DTE2 campaign were obtained in T-rich plasmas, with deuterium NBI and $\omega=\omega_{c,D}$ ICRH.

The evolution of the world fusion energy record pulse (JPN 99971) is shown in Figure 11. The plasma was heated by ~29 MW of NBI and ~4 MW of ICRH power, and ~10 MW of fusion energy was generated for 5 seconds. The discharge was stable and did not suffer from impurity accumulation, central cooling nor adverse MHD as can be seen from the T_e, T_i and radiated power traces. In this plasma scenario, fusion performance is dominated by D_{NBI}-T_{target} reactions. In addition, $\omega=\omega_{c,D}$ ICRH accelerates the bulk and NBI deuterium ions to energies in the range 10-200 keV

an optimum for D-T fusion reactions. From CYRANO-ETS modelling and taking into account slowing down and power redistribution of the RF accelerated deuterium, the fusion power gain with ICRH is estimated to be ~2.5 MW (25%) in this case [32].

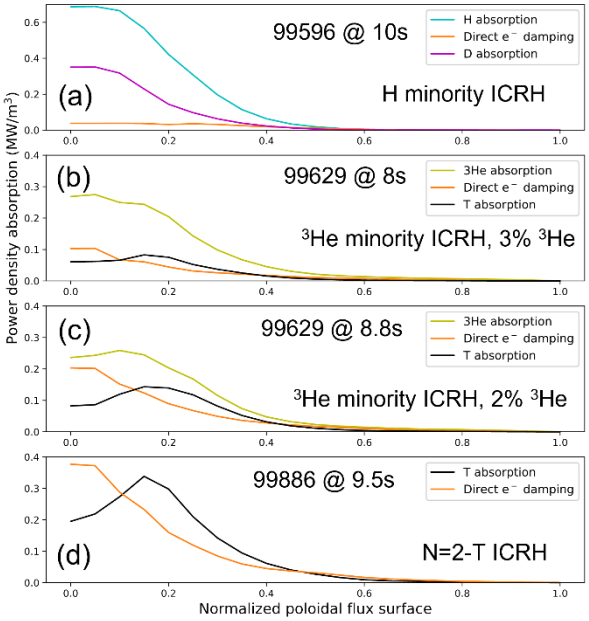

FIGURE 8. RF power absorption profiles from PION simulations. (a) reference with hydrogen minority ICRH (3.5% H); (b) $\omega=\omega_{c,3He}$ ICRH and 3% ^{3}He; (c) $\omega=\omega_{c,3He}$ ICRH and 2% ^{3}He; (d) $\omega=2\omega_{c,T}$ ICRH (0% ^{3}He).

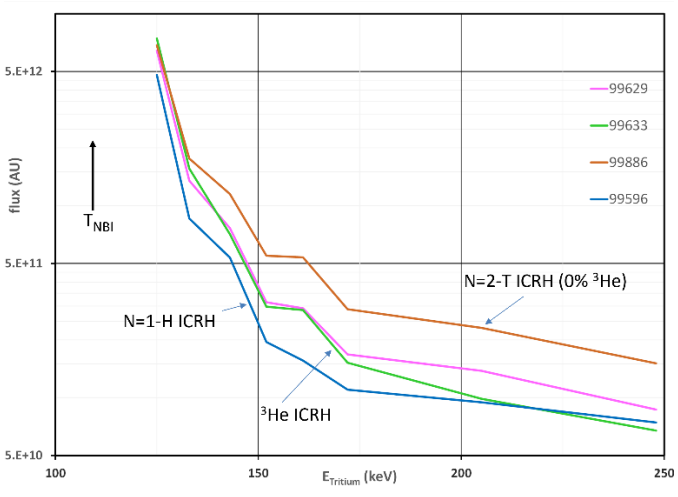

FIGURE 9. NPA fast tritons flux vs energy averaged over 8-9 sec. 99886 pure $\omega=2\omega_{c,T}$ ICRH; $\omega=\omega_{c,3He}$ ICRH, 99629 with ~2.5% ^{3}He and 99633 with ~4% ^{3}He; and 99596 reference with hydrogen minority ICRH.

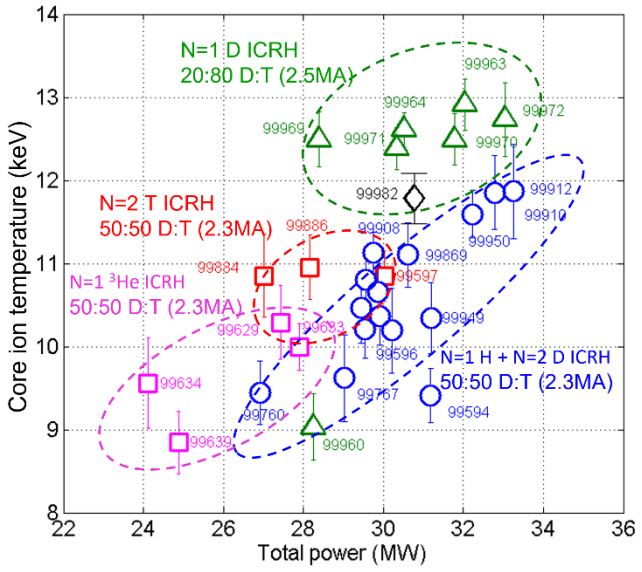

FIGURE 10. Overview of the hybrid-scenario type pulses with different ICRH schemes: Ion temperature (crystal spectroscopy) is plotted vs total heating power, data averaged over 8.5-9.5 sec. Pulses with $\omega=\omega_{c,H}$ ICRH are represented with blue circles. The pure $\omega=2\omega_{c,T}$ ICRH pulses are with red squares and the ones using $\omega=\omega_{c,3He}$ ICRH with magenta squares. The tritium-rich plasmas using $\omega=\omega_{c,D}$ ICRH are with green triangles. 99982 is a 3-ion scheme test reported in [34].

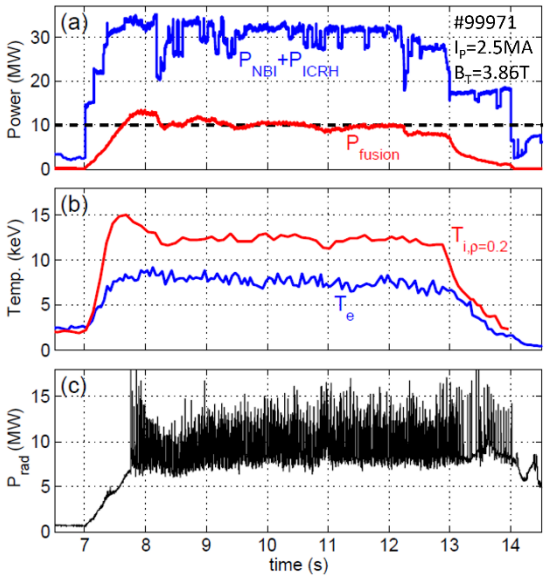

FIGURE 11. Overview of the JET-DTE2 pulse holding the world record for fusion energy, plasma with 20:80 D:T. (a) heating power with D-NBI, $\omega=\omega_{c,D}$ ICRH, and fusion power; (b) central ion and electron temperature; (c) radiated power from bolometry diagnostic.

CONCLUSIONS

Key physics and technology information of direct relevance to prepare ITER operations and that also feed into the design of next fusion reactors were obtained during the JET-DTE2 campaign. Prior to the campaign, a program of enhancements was implemented to adapt the ICRH system and procedures to specific constraints form D-T operations, ensure good availability and reliability of the system and maximize the launched power. Unfortunately, a fault developed in an in-vessel matching capacitor of the ILA on day-2 of the DTE2 campaign, leading to a water leak into the vessel. The leak was isolated and tokamak operations could resume after few weeks, but the ILA was not used for the rest of the campaign. ICRH was used in 80% of the DTE2 campaign pulses; in most of the cases the standard hydrogen minority ICRH scheme was used to provide central plasma electron heating and impurities (especially W) chase-out, contributing to discharges stability. Specific RF-PWI studies were conducted, and it was observed that Be sputtering on the Outer Poloidal limiters was larger in tritium when compared to deuterium; modelling work is ongoing to understand these observations. The ITER DT ICRH scenarios were tested in high performance H-mode plasmas and compared to the standard hydrogen minority ICRH scheme. The plasmas with $\omega=2\omega_{c,T}$ and $\omega=\omega_{c,3He}$ ICRH have increased ion temperature and fusion performance, but these plasmas also suffered from impurity accumulation; this is attributed to the deficit in RF power at the lower frequencies used for $\omega=2\omega_{c,T}$ / $\omega=\omega_{c,3He}$ ICRH and deficit in central electron heating in these specific experiments (note that in ITER, central electron heating will be provided by ECRH). The higher T_i and fusion performance observed with $\omega=2\omega_{c,T}$ and $\omega=\omega_{c,3He}$ ICRH is consistent with the fact that RF accelerated tritium and ^{3}He predominantly slow down on bulk ions; modelling activities integrating RF-plasma codes and transport codes are ongoing to verify that the predicted ion/electron temperatures and fusion performances are in line with the experimental observations. During JET-DTE2, best fusion performances were obtained in T-rich plasmas using D_{NBI} and $\omega=\omega_{c,D}$ ICRH. In these conditions, the beam-target fusion reactions are maximized and deuterium acceleration by the RF wave is optimum for bulk ion heating and for D-T fusion reactions. However, for ITER, a careful assessment of ICRH damping on α particles is still required to conclude on the applicability of this ICRH scenario.

The 3-ion scheme D-(Be)-T was also tested during JET-DTE2, the subject is covered in [34]. Finally, the JET DT and tritium pulses were followed by a cleaning campaign to recover tritium from the vessel and plasma facing components; ~60 ICWC [35] pulses were performed during this phase, totalizing ~915 seconds plasma-time and contributing to the recovery of tritium from the JET vessel.

ACKNOWLEDGMENTS

See the author list of J. Mailloux et al., Nuclear Fusion 62, 042026 (2022) for the list of JET Contributors. This work has been carried out within the framework of the EUROfusion Consortium, funded by the European Union via the Euratom Research and Training Programme (Grant Agreement No 101052200 - EUROfusion) and from the EPSRC (grant number EP/W006839/1). Some part of this work has also been carried out within the framework of the Contract for the Operation of the JET Facilities and has received funding from the European Union's Horizon 2020 research and innovation programme. Views and opinions expressed are however those of the author(s) only and do not necessarily reflect those of the European Union or the European Commission. Neither the European Union nor the European Commission can be held responsible for them.

REFERENCES

1. E. Lerche et al., Nucl. Fusion **56** 036022 (2016).
2. D. Van Eester et al., these proceedings.
3. M. Graham et al., Plasma Phys. Control. Fusion **54** 074011 (2012).
4. I. Monakhov et al., Nucl. Fusion **53** 083013 (2013).
5. I. Monakhov et al., 22nd Topical Conference on Radio-Frequency Power in Plasmas (2017), https://doi.org/10.1051/epjconf/201715703035
6. F. Durodié et al., Plasma Phys. Control. Fusion **54** 074012 (2012).

7. A. Czarnecka et al., Plasma Phys. Control. Fusion 61 (2019) 085004 (11pp)
8. F. W. Perkins et al., Nucl. Fusion **29** 583–592 (1989)
9. J. Myra, J. Plasma Phys. (2021), 87, 905870504
10. V. Bobkov et al., Nuclear Materials and Energy Vol. 18, January 2019, Pages 131-140.
11. A. Krivska et al., Nuclear Materials and Energy, Vol. 19, May 2019, Pages 324-329.
12. V. Bobkov et al., Nuclear Materials and Energy, Vol. 12, August 2017, Pages 1194-1198.
13. D. Milanesio et al., Nucl. Fusion **49** 115019 (2009).
14. ITER Research Plan 2018 ITER Technical Report ITR-18-03
15. D. Van Eester et al., 2002 Nucl. Fusion **42** 310.
16. R. J. Dumont et al., 2013 Nucl. Fusion **53** 013002
17. D.F.H. Start et al., 1999 Nucl. Fusion **39** 321
18. L.-G. Eriksson et al., 1999 Nucl. Fusion **39** 337
19. G. Taylor et al., Plasma Phys. Control. Fusion **38** (1996) 723–750
20. J. Jacquinot et al., 1999 Nucl. Fusion **39** 235
21. A. Murari et al., 2016 IEEE Transactions on Nuclear Science **63** (3).
22. J. Figueiredo et al., 2016 Rev Sci Instrum. **87**, 11D443.
23. S. Vartanian et al. Fusion Engineering and Design 170 (2021) 112511.
24. K. Kirov et al., these proceedings.
25. L-G Eriksson, T Hellsten and U Willén, 1993 Nucl. Fusion **33** 1037
26. K. R.J. Hawryluk, "An Empirical Approach to Tokamak Transport", in Physics of Plasmas Close to Thermonuclear Conditions, ed. by B. Coppi, et al., (CEC, Brussels, 1980), Vol. 1, pp. 19-46
27. Brambilla M. 1994 Nucl. Fusion 34 1121
28. P. Lamalle, PhD thesis, Univ. de Mons (1994); LPP-ERM/KMS report 101
29. P. Strand et al., 2018 Towards a predictive modelling capacity for DT plasmas: European Transport Simulator (ETS) verification and validation. IAEA CN-258, Gandhinagar, India, TH/P6-14.
30. J. Hobirk et al., 2012 Plasma Phys Control Fusion vol.54 095001
31. J. Hobirk, C. Challis, A. Kappatou, E. Lerche et al., 'JET Hybrid scenario for high fusion performance in DT', to appear in Nucl. Fusion special issue on T and DT JET results, 2023.
32. E. Lerche et al., these proceedings.
33. P. Sirén et al., 2022 JINST **17** C08006.
34. Y. Kazakov et al., these proceedings.
35. T. Wauters et al., J. Nucl. Mater. **463** (2015) 1104–1108.